Hindawi
Geofluids
Volume 2019, Article ID 7039165, 16 pages
https://doi.org/10.1155/2019/7039165

Research Article

Hydrogeology and Hydrogeochemistry of the Lauria Mountains Northern Sector Groundwater Resources (Basilicata, Italy)

Filomena Canora,[1] **Giovanna Rizzo**,[2] **Simona Panariello**,[3] **and Francesco Sdao**[1]

[1]*School of Engineering, University of Basilicata, 85100 Potenza, Italy*
[2]*Department of Science, University of Basilicata, 85100 Potenza, Italy*
[3]*Lucanian Aqueduct SpA, Chemistry Division, 85100 Potenza, Italy*

Correspondence should be addressed to Filomena Canora; filomena.canora@unibas.it

Received 13 November 2018; Revised 20 January 2019; Accepted 19 February 2019; Published 28 April 2019

Guest Editor: Ariadne Argyraki

In this study, the hydrogeological characterization of the northern sector of the Lauria Mounts carbonate hydrostructure (southern Apennines, Basilicata region) has been carried out and the hydrochemical properties of different collected groundwater samples have been characterized. Several normal springs drain the hydrostructure, some of them characterized by high annual mean discharges. Groundwater samples were collected from different springs; many parameters such as pH, electrical conductivity, and total dissolved solids have been measured, and major (cations and anions) elements and stable isotopes have been analysed following standard test procedures. Other chemical characteristics were derived from the analysed quality parameters. The results elucidate that the main hydrogeochemical processes control the chemical content and assess the quality of the groundwater within the hydrostructure. The analyses highlight that the chemical compositions of groundwater are strongly influenced by the lithology, especially limestones and dolomitic limestones; they explain and confirm the hydrogeological setting of the system. The groundwater system displays light different geochemical signatures. The processes contributing to the concentrations of major ions depend primarily on carbonate dissolution. The analysis, in all studied groundwater samples, shows that the facies groundwater type is Ca–HCO_3, bicarbonate is the dominant anion, and calcium is the dominant cation with appreciable magnesium concentrations. To identify the aquifer's recharge areas, the environmental stable isotopes oxygen and hydrogen, deuterium, and ^{18}O were analysed. The unaltered $\delta^{18}O$ and δD signatures for the groundwater of the major springs allows identifying the recharge area of these emergencies at elevations ranging from 900 m to 1000 m (a.s.l.), pointing out the presence of deeper flow regime feeding of these springs. The groundwater sample isotopic characteristics of D and ^{18}O suggest that most of the groundwater is recharged directly by infiltration in a high-permeability medium.

1. Introduction

In Mediterranean countries, water availability is a key factor for social and economic development. Recent changes in demography and lifestyle, agricultural land use and irrigation, tourism development, and climate change projections point to an increase in water scarcity and environmental problems with negative implications towards current and future sustainability [1–3]. The balance between water demand and water availability has reached critical levels in many regions; for this reason, a sustainable approach to water resource management is required. This is able to consider the interactions among climate change impacts and water scarcity, surface water and groundwater pollution, and water engineering and human systems including societal resilience and adaptations [4, 5]. Groundwater represents important freshwater resources, used as drinking water supply for agricultural and industrial purposes. Climate variability and human change affect groundwater systems contributing to the decrease in water availability, both directly through modifications in aquifer recharge and indirectly through changes in groundwater quality and use [6]. According to the European and Italian Laws [7–9] on the protection of groundwater against deterioration and

pollution, it is necessary to apply the most appropriate actions and procedures at the hydrogeological basin scale. These actions, finalized to define strategic sustainable management processes, must be able to prevent or contain the potential depletion and pollution of groundwater resources, also taking into account mitigation strategies for climate change impacts [10, 11].

These precious resources, widely exploited, are not distributed at regional level and within each country, in a homogeneous way. The increase in groundwater exploitation poses a severe risk to the availability of the water resources, and the resulting resource scarcity is a major concern in most countries of the Mediterranean region.

Thus, in the last decades, many researches and studies have been planned, devoted to the assessment of the groundwater quantity, quality, and trends. The hydrogeological and groundwater hydrogeochemical assessments have a primary importance to define the hydrogeological conditions of the systems for implementing a sustainable integrated management of groundwater.

Hydrochemical characteristics and stable isotope compositions of groundwater provide important data regarding the water–rock interaction along flow paths, groundwater mixing due to different aquifers and hydrological processes, and area and timing of groundwater recharge for the comprehensive understanding of the hydrodynamic and hydrogeological setting [12–15]. In particular, stable isotopes of oxygen and hydrogen (δ18O and δD) are useful as space tracers of hydrological processes in aquifers, to determine the elevation and conditions of the recharge areas [16–18].

In the Basilicata region (southern Italy), extensive karst and fractured carbonate hydrostructures due to their peculiar geostructural features and hydrogeological conditions are characterized by the presence of a considerable number of springs of good quality.

In order to contribute to an improved understanding of the hydrogeological setting and the groundwater hydrogeochemical characterization of the still poorly understood carbonate hydrostructure of the Lauria Mountains northern sector (southern Apennines), a comprehensive methodological approach was applied. Investigations included geological and hydrogeological field studies to understand the specific characteristics of the hydrogeological system, groundwater sampling at the springs, and chemical analysis of the major elements and stable isotopes (δ18O and δD) to define the hydrogeochemical processes and the recharge area of the major springs.

This will help to provide insight and support in defining groundwater appropriate development actions and strategies, into comprehensive, sustainable, and efficient water resource assessment and management to overcome the future and increase freshwater demands, during the drought periods and in a changing climate scenario.

2. Study Area

The morphostructure of the northern sector of the Lauria Mounts, geographically located along the Calabrian-Lucanian regional border, in the southern-western part of the Basilicata region, is oriented in the W-E direction from Lauria to Castelluccio villages. It is bordered by the watershed of the Sinni River to the N, by the Torrente Peschiera to the NE, and by the urban areas of Castelluccio Superiore and Castelluccio Inferiore to the E. The Mercure River basin bounds the carbonate massif in the SE sector, the Valico Prestieri and Fosso Mancosa in the southern sector, Serra La Nocara to the SW by the Lauria urban area, and the lower part of the Torrente Caffaro tributary of the Noce River to the W. The morphostructure includes the reliefs of La Spina (1652 m) and Zaccana (1580 m) Mounts, Castello Starsia (1387 m), Serra Rotonda (1285 m), and Serra Tornesiello (1185 m) (Figure 1).

The geographic location of the study area, immediately inside the imposing Apennine Chain, which rises along the Tyrrhenian coast, has a strong impact on climate factors. The nearness to the sea confers its beneficial effect to the climate which results to be substantially mild, despite the elevations of the territory, with a very high average annual precipitation of about 1550 mm. The annual typical Mediterranean rainfall regime involves very rainy winters and dry summers. The maximum monthly precipitation value is recorded in December, the minimum in July. The regime of temperature is essentially characterized by the mean maximum value of about 23°C in summer that always occurs in the months of July-August and the mean minimum value of about 6.5°C in winter. The average annual temperature is instead about 14°C. The hydrographic network is mainly present on the carbonate rocks that form the central structure and on the alluvial deposits characterized by good permeability and low slope gradients. The development of minor streams is controlled by the state of fracturing of the carbonate and is distributed around several directions.

The straight segments of streams (e.g., Torrente Caffaro, Fosso Mancosa) are strongly related to the main fault systems that evidently have conditioned the hydrographic network development. In the SE edge of Serra Rotonda, a small lake, Lago La Rotonda, with a seasonal regime is located in a small endorheic basin; it has a water-extended surface in rainy months and dry in the summer. The lake is generated in correspondence of a karst polje, in which, at the bottom, detritical and palustrine deposits are present. The morphostructure hosts an important carbonate hydrostructure, drained by many springs some of which are characterized by huge groundwater discharges.

3. Geological Setting of the Lauria Mounts

The Lauria Mountains consist of a series of ridges, coincident with morphostructures with a N120° SE pattern, located to the west of the Mercure Basin, which separates them from the neighbouring mountains of the Pollino Chain and represents the link between the Campanian-Lucanian Apennine and the domains belonging to the crystalline-metamorphic sedimentary rocks of the Calabrian-Peloritan Arc.

The Lauria Mountains, characterized by a significant geological and structural complexity, represent a high structure consisting of the Meso-Cenozoic calcareous-dolomitic succession, referable to the Alburno-Cervati-Pollino Unit

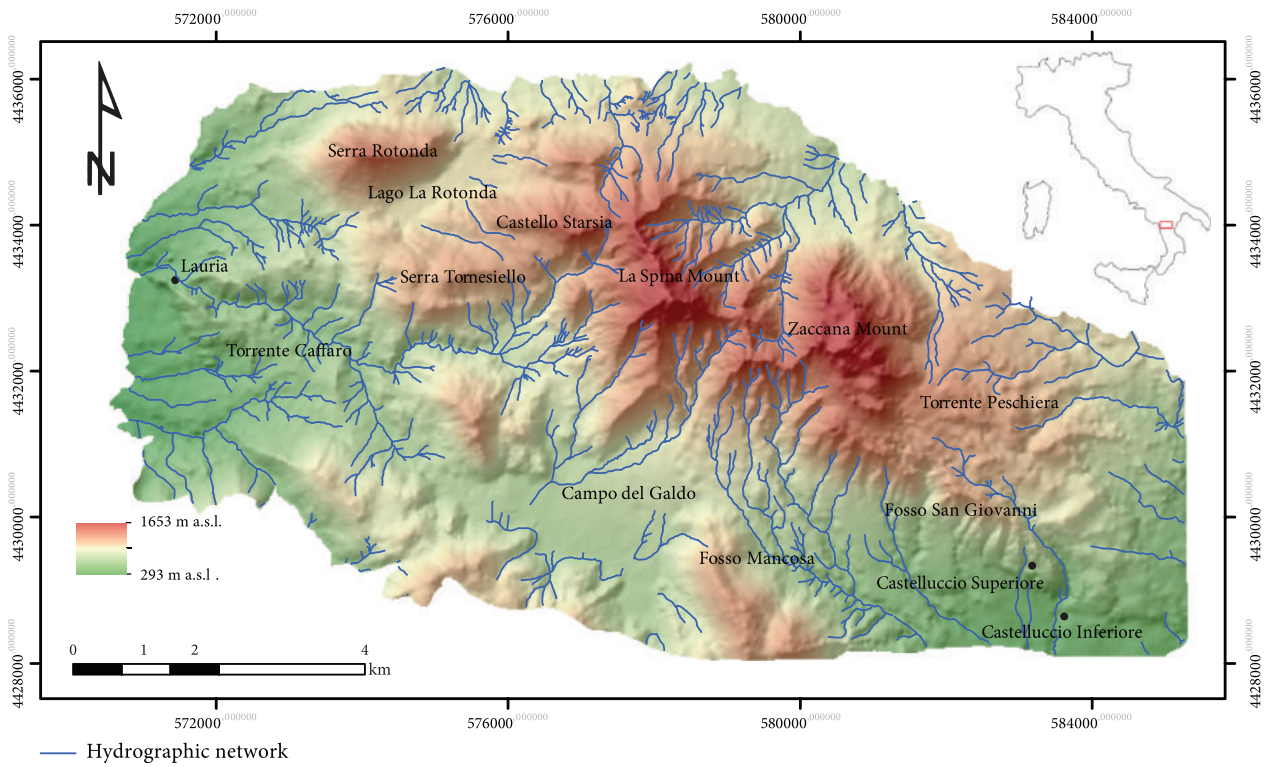

Figure 1: Geographic location, digital elevation, and hydrographic network of the study area.

[19], constituting the monoclines of the Calabrian-Lucanian border, confined by the Miocene argillite-marly flysch.

In particular, in the Lauria Mountains it is possible to distinguish the Lauria-Castelluccio northern ridge, consisting of the main reliefs of Castello Starsia, Serra Rotonda, La Spina, and Zaccana, where carbonates, from Triassic to Cretaceous, such as dolomites, dolomitic limestones, and limestones constitute the central structure, while terrigenous sediments are present along the lower part of the northern slopes. Quaternary sediments organized in different continental depositional environments fill the southern sector. This morphostructure is separated from the southern Trecchina-Laino ridge by a tectonic line with a transcurrent trend oriented N110°-120° that has cut the existing plicative structures. Cretaceous limestones of the Serra San Filippo and Serra La Nocara reliefs and Jurassic-Cretaceous limestones of the Rossino and Fossino Mounts constitute the southern morphostructure.

The morphodynamic evolution of the Pollino Chain and Lauria Mountains has been highly controlled by the transcurrent and distensive Plio-Quaternary fragile tectonics [20–22].

The transcurrent deformation, active from the Upper Pliocene, whose faults are subsequently reactivated in the extensional system [22, 23], produces a complex structural pattern [24]. Several geological and structural studies of the entire area [21, 23, 25] made it possible to place a time constraint to the transcurrent activity, which is still present during the Sicilian, while the extensional tectonic, still active, develops starting from the passage between the Lower and Middle Pleistocene.

The tectonic structures oriented approximately N120° are extremely important, as responsible for the genesis and evolution of many quaternary basins, including those present in the Calabrian-Lucanian border [22].

The morphostructure of the northern sector of the Lauria Mountains, oriented in the WNW-SSE direction, is located to the north-west sector of the Mercure Basin, which separates the carbonate structure from the neighbouring mountains of the Pollino Chain [26].

The study area highlights different fault systems, with predominantly Apennine faults orientation N120 ± 10° and distributed fault systems oriented N-S and N30°-50°, generally in association with thrusts and folds [26] (Figure 2).

The carbonate morphostructure is bordered by high-angle transcurrent and extensional faults that generated a series of depressions filled by Quaternary continental deposits and by Miocene terrigenous deposits [25]. Carbonate successions are bounded to the north by an important thrust front with N-NE vergence, produced by the translational tectonics that led Liguridi and Sicilidi-Affinity Units to overlap on Carbonate Units of the Apennine Platform and on Lagonegresi Units [27].

The presence of the fault with NNW-SSE direction, which plunges to WSW with a fault throw of about 400 m, divides the limestone-dolomitic area in two zones, the first one to the west and the second to the east of the mentioned fault.

This fault starts from Lago La Rotonda and, passing between Castello Starsia and the right side of Serra Tornesiello, reaches Campo del Galdo, in correspondence

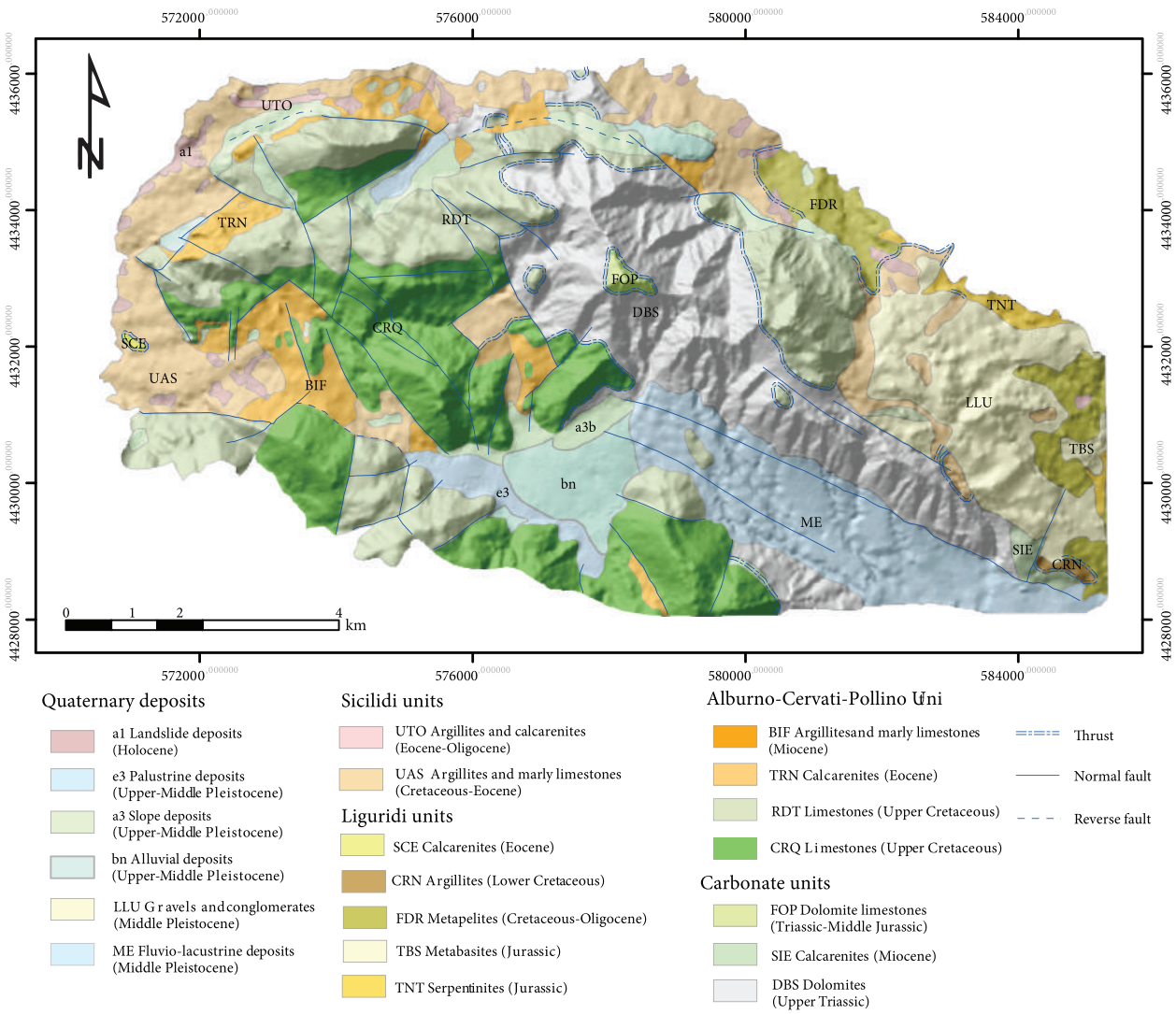

Figure 2: Geological map of the Lauria Mountains northern sector (adapted from ISPRA, 2016 [31]).

to the base of the western slope of the La Spina Mount. A network of normal faults characterized by three main systems with NNW-SSE, SW–NE, and E-W directions, globally affects and lowers the western area of this fault.

In the study area are different distinguishable stratigraphic-tectonic units that constitute the structure of the Lucanian Apennines [19] (Figure 2).

Lagonegresi Units, outcropping only limited along the northern external borders of the morphostructure, represent the sedimentary succession of the Lagonegrese Basin [28] constituted, from the bottom to the top, by the Monte Facito Formation (Lower-Middle Triassic), the Cherty Limestone Formation (Upper Triassic), the Siliceous Schist Formation (Cretaceous-Jurassic), and the Galestri Formation (Jurassic Superior) [27, 29–31].

Carbonate Units of the Campanian-Lucanian Platform, represented by the calcareous and calcareous-dolomitic Mesozoic succession [32], overlay the Lagonegro Units. Carbonate Units constitute the entire structure of the Lauria Mountains. Carbonate successions belong to the tectonic units of the Maddalena Mounts and Foraporta Mount and to the Alburno-Cervati-Pollino Unit and comprehend, from the bottom to the top, red shales and cherty limestone of the Middle Triassic, followed by a powerful succession of dolomites (Upper Triassic) and limestones, with subordinate marls [32].

Liguridi Units, present in the area surrounding the northern morphostructure of the Lauria Mountains and extensively to the north-east sector of Castelluccio Superiore, include the turbidite succession of the Liguride Complex (Cretaceous-Oligocene) [33–35].

It represents the remaining part of an accretionary wedge, subsequently divided into two tectonic units: the metamorphic Frido Unit and the unmetamorphosed Cilento Unit [19, 29, 36, 37], which include the Crete Nere, Saraceno (north-Calabrian Units), and Albidona Formations (intra-Chain Basin Deposits) [38]. At these formations are tectonically overlapping deposits ascribed to the "Sicilide Affinity Units," made up of marly, calcarenite-clayey, and arenaceous-pelitic deposits (Upper Cretaceous-Oligocene);

the Torbido River Unit, consisting of marly and calcilutite limestone with nodules of chert, calcarenites, sandstones, and red argillites (Middle-Oligocene Eocene), stands above tectonically to these deposits [39].

The aforementioned deposits appear to be those geometrically higher than the south-Apennine Chain and mainly outcrop along the western border of the morphostructure, at N and NE of Serra Rotonda.

Quaternary deposits include different clastic deposits such as gravelly-sandy and subordinately sandy-loamed deposits, as well as clayey and marly continental sediments of the Noce and Mercure fluviolacustrine basins. These deposits are present mostly in the SE part of the study area attributable to different accumulation phases and intercalations of paleosols formed by brown silty clays with skeletons of different sizes, which testify to repeated periods of stasis in alluvial sedimentation. Sandy-gravelly deposits, colluvial deposits, and detrital cones of the Upper Pleistocene-Holocene outcropping almost everywhere along the southern slopes of the hydrostructure form a series of alluvial fan deposits that are interdigitated to the middle-Pleistocene lacustrine deposits of the Mercure Basin [22].

4. Hydrogeological Characterization of the Carbonate Hydrostructure

4.1. Geomorphological and Structural Factors' Role on the Aquifer System. The geostructural and geomorphological peculiarities of the morphostructure strongly affect the complex hydrogeological setting of the hydrostructure, the groundwater flow directions, and the presence of the springs.

The carried-out hydrogeological and hydrogeochemical surveys highlight that the geometrical configuration of the carbonate hydrostructure of the Lauria Mounts northern sector is structured according to different carbonate aquifers. Major faults and karst or fracturing conditions define the hydrogeological watersheds, to places with underground water interchanges, with different hydrogeological and hydrodynamic characteristics, and organize in the carbonate rocks' distinct groundwater flow patterns.

Based on the distinct geolithological, structural features and relative permeability of the stratigraphic-tectonic units, different hydrogeological complexes have been distinguished in the study area [40], each of them characterized by common spatial arrangement, prevalent permeability, and a degree of relative permeability restrained in a narrow range [41].

Limestones, dolomitic limestones, and dolomites constitute the Carbonate Complex that host the most important aquifers drained by the springs with major discharge amounts. It can be divided into three subcomplexes depending on the presence or absence of the karst process and forms (dolines and cavities) and the density of rock fracturing state; the hydraulic conductivity ranges from 10^{-4} m/s to 10^{-2} m/s [42], and the relative permeability varies from medium-high to very high, representing the favoured complex for the infiltration.

The Conglomerate Complex, mainly outcropping in the south-eastern part of the investigated area, consists of conglomerates and breccias. Characterized by a medium-high degree of relative permeability, it presents a discrete groundwater flow fed by the carbonate complexes. This complex stores part of the groundwater amount and allows the emergence of smaller springs.

The Calcarenite Complex, made of a gray well-layered calcarenite succession with frequent intercalations of marls, has a subordinate role in the local hydrogeological framework, which presents a medium degree of relative permeability due to the presence of the rock fractures.

The Detritical Complex, constituted by heterogeneous conglomerates and gravels with different cementation degrees, includes the detritical and clastic deposits that constitute the alluvial fans and the debris cones. Its hydraulic conductivity ranges from 10^{-7} m/s to 10^{-5} m/s with a medium degree of relative permeability [42].

The Fluviolacustrine Complex, characterized by a medium-low degree of relative permeability, comprehends clays, marly clays, layered clayey marls with sandy layers, and polygenic conglomerates rich in sandy matrix. It is largely made up by the quaternary deposits of the Mercure Basin that borders the carbonate hydrostructure along its southern boundary.

The Clayey-Marly Complex includes pelagic and chaotic sequences of varicoloured clays, marls, and marly limestone, belonging to the Sicilidi-Affinity and Lagonegresi Units and quartzites; clays and marls referable to the Frido Unit, in which even ophiolitic elements can be distinguished [43–45]; and arenaceous-pelitic alternation belonging to the Flysch of Albidona. This complex has a low degree of relative permeability, borders the carbonate hydrostructure, and plays an important hydrogeological role representing the limit of permeability in some parts of the system; the hydraulic conductivity is $<10^{-9}$ m/s [42].

The geometry of the carbonate hydrostructure and the underground watershed are mainly defined by the structural elements present throughout the entire hydrostructure, such as faults and thrust, tectonic deformation bands, and karst and fracturing state of rocks.

The assessment of the karst phenomena in the area was based mainly on the recognition of the surface karst forms; the entity of the underground karstic development is evinced considering the geomorphological context and the spring's emergency areas that leads to the consideration of the presence of evolved fractures and karstic conduits. The presence of the karst morphologies, on the dolomitic limestones, suggests a local prevalence of the calcareous component on the dolomite. They represent the surface trace of a developed underground karst network.

This specific hydrogeological setting bordered laterally by major faults and characterized by subsurface boundaries, due to tectonic elements, lithological arrangement, and development of karst network, influences the different groundwater flow directions and the emergence of numerous springs, distinguishing two aquifers with different hydrogeological and hydrodynamic characteristics (Figure 3).

The Lauria and La Spina-Zaccana aquifers, both characterized by the presence of important springs, located in the western and eastern parts of the carbonate massif, at altitudes between 315 m and 504 m a.s.l., represent strategic

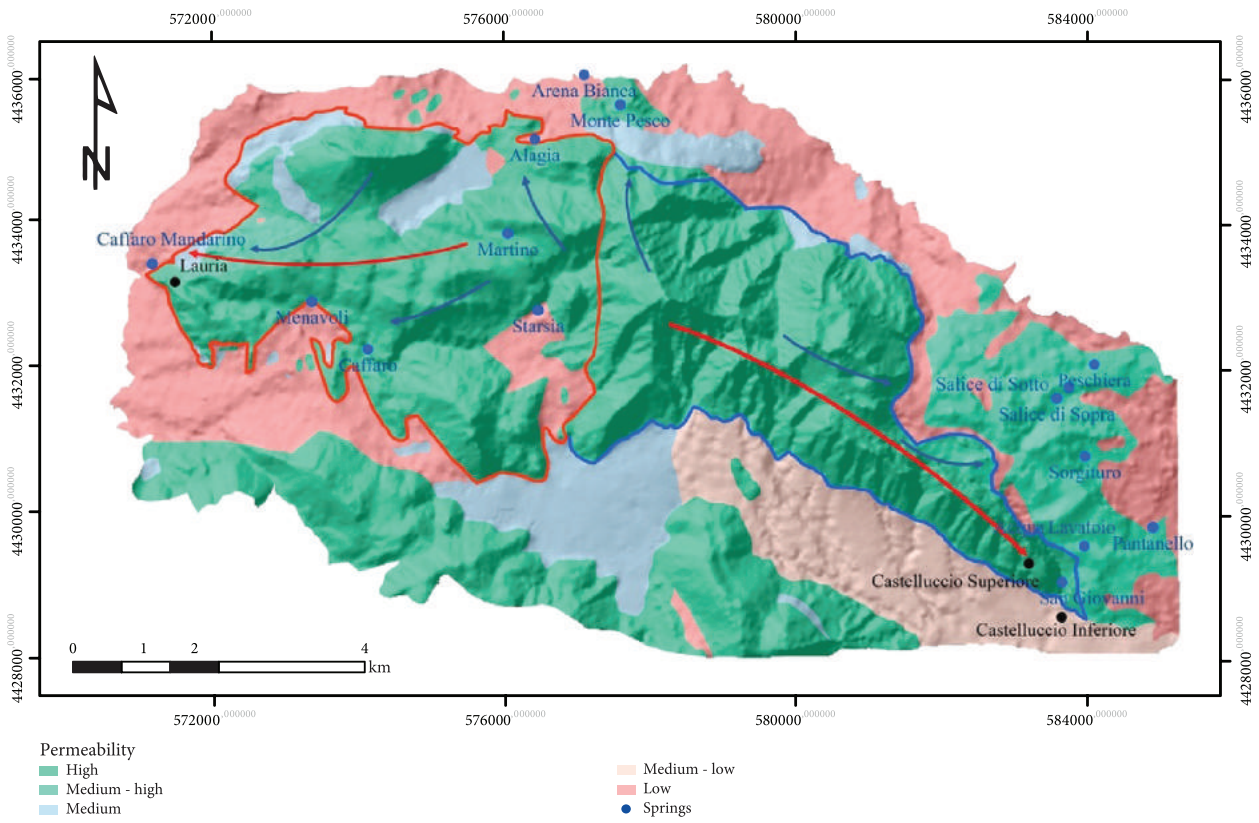

Figure 3: Hydrogeological map showing Lauria Aquifer (red line) and La Spina-Zaccana Mounts Aquifer (blue line) with relative permeability classes, main groundwater flow directions (red arrows and blue arrows represent, respectively, deep and shallow groundwater flow pathways), springs, and main urban areas (black circle).

water resources for the area and for the Basilicata region. Several other emergencies with smaller groundwater amounts are present along the border of the carbonate hydrostructure (Figure 3).

The groundwater flow, conditioned by different factors such as tectonic arrangement, rock fracturing degree, karst activity, and presence of the basal dolomite complex at the south-eastern part of the aquifer system, essentially occurs in two preferential directions.

The prevailing NE-SW and NW-SE directions are oriented towards the areas where the major springs emerge, most of which are not adequately exploited or even uncollected.

4.2. Hydrogeological Features of the Lauria and La Spina-Zaccana Aquifers. The Lauria Aquifer is characterized by an evident stratigraphic-structural complexity. The carbonate structure is affected by a dense network of high angle direct faults, which develop the geometry of en-echelon from Lago La Rotonda to Campo del Galdo. This direct fault system shows a vertical fault throw of at least 400 meters and gets down the entire western block of the Lauria Ridge with respect to the La Spina-Zaccana Ridge.

The most evident consequence of this remarkable dislocation is represented by the difference of the lithological outcrops between the two blocks: in fact, while the limestones outcropping mainly characterizes the lowered western block of the Lauria side, the eastern block is largely constituted by the outcrops of the deepest dolomitic limestones and dolomites.

In correspondence of this fault system, the distribution of the layered carbonate succession defines an anticlinal fold with the axial zone localized between Castello Starsia and La Spina Mount; it can be considered the tectonic structure that presumably corresponds to the hydrogeological watershed between the two aquifers.

Argillite-marly flysch and clayey-marly flysch bound, to the north and to the west, the carbonate aquifer, consisting limestones and dolomitic limestones. Argillite and marly limestones outcrop to the south, and the most markedly dolomitic terms emerge to the east characterized by an intense fracturing state. The groundwater pathways, influenced by the presence of different faults, has the preferential flow direction oriented NE-SW. It starts from the hydrogeological watershed with the La Spina-Zaccana aquifer and is directed towards the main emergencies located at W of the hydrostructure. The main springs, located in the municipality of Lauria, such as Caffaro-Mandarino, Caffaro, and Arena Bianca, reach a total capacity of about 845 $L\,s^{-1}$ [46].

The three different important emergencies of Caffaro-Mandarino with the flow rate of about 0.81 $m^3\,s^{-1}$ [46], located on the edge of the carbonate structure, is tamponed by the clayey-marly flysch formations of the Sicilidi-Affinity Unit. The group of Caffaro-Mandarino springs represents

the delivery points of the deep aquifer groundwater flow. Nowadays, its discharge is partly used for hydroelectric purposes.

The Caffaro Spring did not naturally emerge, but the derivation of the draining tunnel was realized for a hydroelectrical system; the flow rate of the Caffaro is equal to $25\,L\,s^{-1}$ [46]. Some quantities of water flow in the detritical deposits or feed the minor springs: Alagia, Martino, and Montepesco, placing a different altitude, refer to shallow underground water circuits that characterize the variable regime of the small flow rates. Those positioned on average from 645 to 1120 m a.s.l. are located in two distinct areas enclosed between the northern slopes of Castello Starsia and the southern side of Serra Tornesiello. Starsia and Menavoli springs with $4\,L\,s^{-1}$ flow rates are used for local needs (Figure 3). The presence of some springs at the northern edge of the hydrostructure is due to the underground water transfers of the carbonate rocks towards the flysch deposits in the most permeable areas and towards the detrital cover.

The La Spina-Zaccana aquifer constitutes the central-eastern portion of the northern area of the Lauria Mountains and consists of the two reliefs of La Spina and Zaccana Mounts.

The dolomites and dolomitic limestones represent the dominant geological formations and are constituted, at the bottom, by a monotonous succession of gray and micro- and macro-crystalline dolomites. Fluviolacustrine deposits of the Mercure Basin and a series of continental quaternary deposits, mainly present in the southern boundary of the aquifer and in some peripheral sectors of the La Spina-Zaccana ridge, are represented by coarse and subordinately fine clastic sediments, consisting of clays and marls.

Although dolomitic limestone and dolomite are considered part of a single succession in original stratigraphic continuity, a band of intense cataclastic deformation is evident at their contact, which is therefore to be considered of tectonic type. It has already been recognized in the study area [20, 47] and interpreted as a low-angle tectonic contact with a predominantly extensional or transtensive kinematics of a *younger on older* [48]. The carbonate aquifer is bounded almost in all directions by exclusively tectonic contacts of different nature and kinematics and stratigraphic places.

The north-western boundary of the hydrostructure is located in the anticlinal hinge zone of the Castello Starsia-La Spina Mount. At its north-eastern edge, however, the aquifer is bounded by a thrust, to places lowered by some normal faults, which superimposes the argillite-marly formations on the carbonates. Along the southern edge, the La Spina-Zaccana substructure is bounded by an important fault, indicated as Castelluccio Fault, with high inclination, oriented in the N120° direction and submerged towards SSO. It is formed in the Pleistocene with a left transcurrent kinematics subsequently reactivated as a direct fault in the upper Pleistocene.

The high and steep slope that characterizes the southern side of the La Spina-Zaccana ridge morphologically highlights the high rate of activity of this fault and its considerable vertical throw. Within its limits, the La Spina-Zaccana morphostructure does not seem to be crossed by major faults, except for the NS subvertical direct fault present in the southern slope that intersects the Castelluccio Fault and which lowers the eastern sector.

The Castelluccio Fault acts as the morphostructural southern limit of the structure and from a hydrogeological point of view represents the superimposed permeability threshold of the San Giovanni spring front.

The La Spina-Zaccana carbonate aquifer represents significant groundwater resources, well fed and drained in large part from the San Giovanni spring; minor emergencies of less potentiality are scattered throughout the south-eastern sector of the structure (Figure 3).

Along the entire southern slope of the La Spina-Zaccana Ridge, the Castelluccio Fault places in tectonic contact the carbonate rocks of the aquifer with the Pleistocene fluviolacustrine deposits of the Mercure Basin. The geometry of the aquifer, its main hydrogeological characteristics, the underground water circulation, and the groundwater emergencies are closely connected to the geological, structural, and karst arrangement. The recharge area, essentially located at high altitudes of the hydrostructure, includes the main reliefs of the study area, towards the W-E direction.

The groundwater flow, predominantly, in the NW-SE direction, feeds the San Giovanni springs group, Acqua del Lavatoio and Pantanello springs along the eastern edge of Monte Zaccana. These springs have a total flow rate of about $580\,L\,s^{-1}$ [46]. The San Giovanni spring front (at least 7 normal permanent springs) (mean discharge of $450\,L\,s^{-1}$) [46], one of the most important groundwater resources of the Lucanian Apennines, is located along a steep slope at an altitude of between 480 m and 504 m. Groundwater is mainly, if necessary, exploited for drinking purposes and irrigation use. Other water emergencies, such as Peschiera, Salice Sopra, Salice Sotto, and Sorgituro, drain limited surficial aquifers characterized by shallow groundwater flow paths.

4.3. Sampling and Analytical Methods. Groundwater samples were collected from 15 springs, some of them partially used for drinking, irrigation, and hydroelectrical purposes, during a single field trip in May 2017. During the rainy season, another sampling was carried out only for isotopic analyses (November 2017).

The sampling sites, located mainly in the western and eastern sectors of the hydrostructure, were selected based on the complex hydrogeological geometry and hydrodynamic characteristics of the aquifers (Figure 3).

Groundwater springs were sampled to define the main hydrogeological and hydrogeochemical processes controlling the chemical properties. Physicochemical parameters including groundwater temperature, pH, and electrical conductivity were measured in situ. One filtered aliquot (using 0.45 μm cellulose acetate filters) and one filtered and acidified (with HNO_3) aliquot were collected and stored in low-density polyethylene bottles for laboratory analysis of major elements. The major elements were determined by ion chromatography, IC Metrohm 850 Professional. Cations (Na^+, K^+, Ca^{2+}, and Mg^{2+}) were separated by a Metrosep C 4 250/4.0 column using 3.0 mM HNO_3 as eluent and a flow

Table 1: Physicochemical parameters of the groundwater samples.

Spring name	Sample	Est	North	Altitude (a.s.l.)	Discharge (L/s)	pH	EC (μS/cm)	T (°C)
Alagia	P1	576401	4435186	920	2	7.2	550	10.9
Arena Bianca	P2	577083	4436071	735	11	7.7	383	11.6
Martino	P3	576032	4433888	1120	1	7.3	397	9.8
Montepesco	P4	577580	4435661	950	4	7.5	387	10.8
Caffaro	P5	574107	4432297	640	25	7.6	365	10.8
Caffaro M.	P6	571133	4433471	315	810	7.8	369	11.7
Menavoli	P7	573333	4432955	645	2	7.2	498	13.2
Starsia	P8	576448	4432836	835	4	7.4	535	12.7
Acqua Lavat.	P9	583972	4429592	705	4	7.7	430	10.2
Pantanello	P10	584918	4429849	630	16	7.5	425	11.4
Peschiera	P11	584111	4432091	910	4	7.5	390	11.4
Salice Sopra	P12	583759	4431779	925	5	7.5	372	13.4
Salice Sotto	P13	583594	4431623	940	4	7.6	365	13.1
San Giovanni	P14	583670	4429095	504	540	7.6	358	11.2
Sorgituro	P15	583982	4430826	875	3	7.6	365	10.8

Discharge data are from Basilicata Region [36]. The sampling sites are in WGS1984 UTM Coordinate System Zone 33N.

Table 2: Major element concentrations of the spring's groundwater sampled in the study area.

Sample	Na^+ (mg/L)	K^+ (mg/L)	Mg^{2+} (mg/L)	Ca^{2+} (mg/L)	Cl^- (mg/L)	NO_3^- (mg/L)	SO_4^{2-} (mg/L)	HCO_3^- (mg/L)	CS (meq/L)	AS (meq/L)	E (%)	SI calcite	SI dolomite
P1	4.1	0.5	11.8	62.0	4.5	1.0	2.8	251	4.3	4.3	-1.4	-0.3	-1.1
P2	6.1	0.4	13.4	62.8	8.5	4.4	7.6	252	4.5	4.6	-2.1	0.3	0.0
P3	4.4	0.6	8.2	60.1	5.8	0.1	4.6	232	3.9	4.1	-4.6	-0.2	-1.3
P4	3.6	0.5	11.1	58.0	4.4	1.2	3.3	240	4.0	4.1	-4.2	0.0	-0.6
P5	3.9	0.3	16.6	52.0	5.7	1.5	3.5	233	4.1	4.1	1.5	0.0	-0.3
P6	4.8	0.6	13.2	52.0	5.3	2.3	5.0	225	3.9	4.0	-1.6	0.5	0.5
P7	6.3	0.2	4.7	73.0	8.2	1.7	8.0	245	4.3	4.4	-3.0	-0.2	-1.3
P8	5.8	1.4	8.4	62.0	6.9	4.1	9.5	228	4.1	4.2	-2.9	0.0	-0.8
P9	3.9	0.2	18.6	52.8	5.6	1.8	4.6	245	4.3	4.3	1.0	0.2	0.0
P10	5.6	1.4	12.2	66.7	6.2	8.1	5.0	256	4.6	4.6	0.0	0.1	-0.4
P11	3.6	0.5	11.1	62.5	4.7	1.9	3.9	244	4.2	4.2	-1.0	0.0	-0.5
P12	3.6	1.5	12.9	74.2	3.8	0.1	0.8	297	5.0	5.0	-0.7	0.2	-0.1
P13	3.9	0.6	12.7	57.9	5.7	1.7	4.0	233	4.1	4.1	0.6	0.1	-0.2
P14	4.8	0.2	20.1	40.8	7.2	0.1	3.2	220	3.9	3.9	0.9	0.3	-0.3
P15	5.0	0.5	15.0	51.8	7.2	2.9	6.2	224	4.0	4.1	-0.2	0.0	-0.5

rate of 0.9 mL/min, whereas anions (F^-, Cl^-, NO_3^-, and SO_4^{2-}) by a Metrosep A supp7 250/40 column using 3.6 mM Na_2CO_3 as eluent at a flow rate of 0.7 mL/min. Alkalinity was determined by titration with 0.1 N HCl. The analytical precision was always better than 5% for each analysed species, and the ion balance (i.e., the difference between the cations and anions sum) was always within 3%.

The geochemical software PHREEQC 3.0 [49, 50] was used to calculate aqueous speciation of the investigated elements. Saturation index, defined as SI = log (IAP/Kt), IAP being the ion activity product of the mineral–water reaction and Kt the thermodynamic equilibrium constant at the measured temperature, were calculated by ion activities. Thus, SI = 0 indicates a thermodynamic equilibrium state, and values >0 denote oversaturation and <0 undersaturation.

The field chemical composition of the analytical results and the saturation index (SI) values for calcite and dolomite are reported are listed in Tables 1 and 2.

Validation procedures characterize the analytical performance of laboratory tests in order to understand its capability and limitations. The limit of detection and the limit of quantitation (LOD and LOQ) are the parameters used to describe the analytical sensitivity of an analytical procedure.

The detection limit, LOD, represents the smallest concentration of an analyte in a sample that can be detected with reliable statistical certainty under the stated conditions of the

analytical test, with no guarantee about the bias or imprecision of the result.

The value is determined as the analyte concentration corresponding to the sample blank value plus three standard deviations:

$$\mathrm{LOD} = X_{b1} + 3S_{b1}, \quad (1)$$

where X_{b1} is the mean concentration of the blank and S_{b1} is the standard deviation of the blank.

The LOQ is the lowest analyte concentration, determined with acceptable precision and accuracy under the stated conditions of the test, and corresponding to the sample blank value plus ten standard deviations as shown in the following equation:

$$\mathrm{LOD} = X_{b1} + 10S_{b1}, \quad (2)$$

where X_{b1} is the mean concentration and S_{b1} is the standard deviation of the blank.

The weakness is that there is no objective evidence to prove that a low concentration of analyte will indeed produce a signal distinguishable from a blank (zero concentration) sample [51]. Results of the detection and quantification limits of the analyzed elements are expressed in Table 3.

To evaluate the interrelationships affecting the distribution of the major chemical elements, an R-mode factor analysis was performed.

Factor analysis provides a way to reduce the data to an easily interpretable form, by identifying chemical signatures expressed through statistically significant factors determined by the analysis.

R-mode factor analysis was undertaken by the Statgraphics Centurion XVI package [52], and factor component matrix is extracted (Table 4).

This matrix, showing the impact coefficient of the two extracted components, evidences the link between these components and the groups of variables.

The $^{18}O/^{16}O$ and $^{2}H/^{1}H$ ratios were determined by isotope ratio mass spectrometry (IRMS). Oxygen isotope measurements were carried out by using a Gas Bench peripheral coupled with a Thermo Delta V mass spectrometer. A TC-EA peripheral interfaced by means of a ConFlo IV with a Thermo Delta XP mass spectrometer was used for hydrogen isotopes. Results are expressed in terms of *d*-values (i.e., δD and δ^{18}O) with respect to the Vienna Standard Mean Ocean Water (VSMOW) as follows:

$$\delta[‰] = \frac{R_{\mathrm{sample}} - R_{\mathrm{VSMOV}}}{R_{\mathrm{VSMOV}}} \times 1000, \quad (3)$$

where R_{sample} is the stable-isotope ratio ($^{2}H/^{1}H$ or $^{18}O/^{16}O$) of the sample and R_{VSMOV} is the ratio for VSMOW. The analytical error for IRMS was ±0.1‰ for δ^{18}O and better than ±1‰ for δD. The isotopic data of the two sampling periods are reported in Table 5.

Table 3: Detection limit (LOD) and quantitation limit (LOQ) of the major element concentrations.

Element	LOD (mg/L)	LOQ (mg/L)
Na	0.28	0.94
K	0.18	0.67
Mg	0.15	0.49
Ca	0.17	0.56
Cl	0.48	1.61
SO	0.28	1.63
NO	0.1	1.14

Table 4: R-mode factor analysis results.

	Component 1	Component 2
EC	0.125	0.606
pH	-0.101	-0.503
Na^{+}	0.962	0.137
K^{+}	-0.005	0.606
Mg^{2+}	-0.318	-0.571
Ca^{2+}	0.093	0.956
Cl^{-}	0.859	-0.235
NO_3^{-}	0.490	0.223
SO_4^{2-}	0.923	0.039
HCO_3^{-}	-0.343	0.719

Table 5: Stable isotope composition of groundwater collected in two sampling periods.

Sample	δ^{18}O	δD	δ^{18}O	δD
	May 17		Nov 17	
P1	-8.1	-48	-8.8	-54
P2	-8.2	-47	-8.7	-53
P3	-8.2	-49	-8.9	-54
P4	-7.6	-45	-8.6	-53
P5	-7.7	-46	-8.4	-52
P6	-7.8	-46	-8.6	-51
P7	-7.5	-42	-8.4	-52
P8	-7.5	-45	-8.5	-50
P9	-7.5	-44	-8.3	-50
P10	-7.6	-44	-8.2	-52
P11	-7.7	-44	-8.3	-52
P12	-8.4	-52	-8.5	-53
P13	-7.8	-43	-8.4	-50
P14	-8.5	-52	-8.6	-53
P15	-8.6	-53	-8.6	-54

The isotope composition of O and H is reported in δ units per mil vs. the V-SMOW standard. The analytical error was ±0.1‰ for δ^{18}O and better than ±1‰ for δD.

5. Results and Discussion

5.1. Chemical Composition of Groundwater. Groundwater samples are characterized by low electrical conductivity

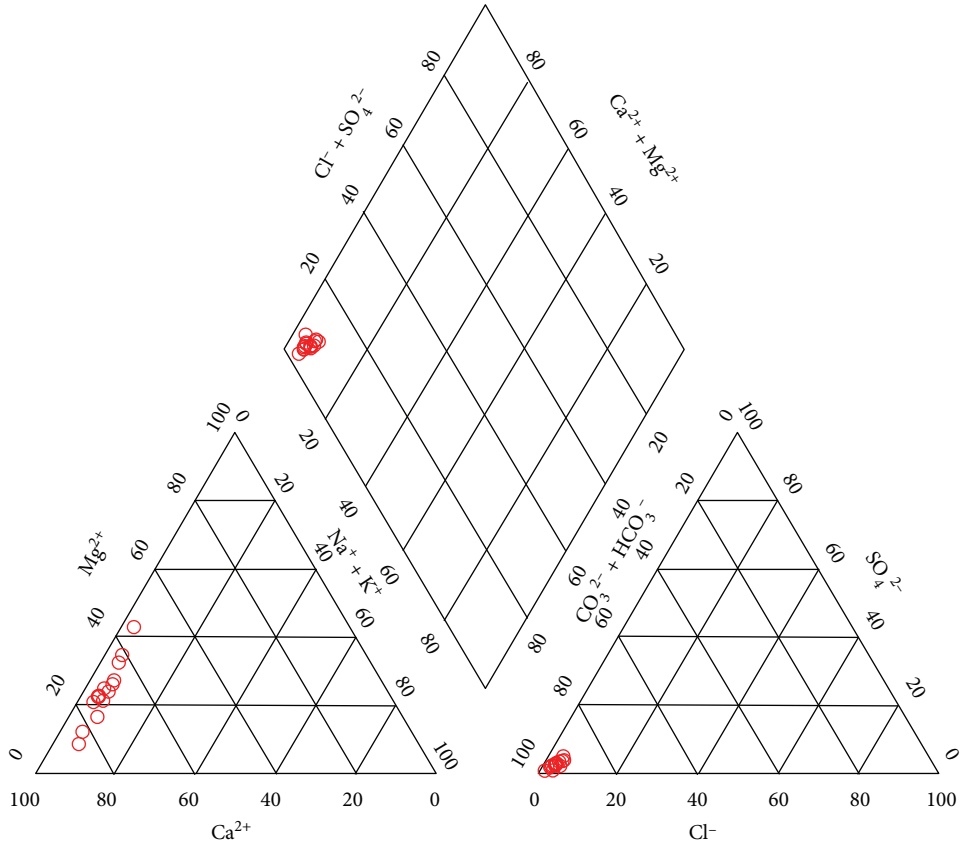

Figure 4: Piper diagram showing the groundwater hydrogeochemical facies.

(EC) values, ranging from 358 to 550 μS/cm, alkaline pH values (from 7.2 to 7.8) and temperature values between 9.8 and 13.4°C. The bicarbonate is the main anion in solution with concentrations ranging between 220 mg/L and 297 mg/L with an average value of 242 mg/L. Calcium and magnesium are the most abundant cations with average values of 59.2 and 12.7 mg/L, respectively.

NO_3 concentrations range from 0.1 mg/L to 8.1 mg/L and are lower than the maximum admissible concentrations defined by the Italian Law [53]. All the sampled groundwater records the following order of abundance in terms of cation and anion concentrations: $Ca^{2+}>Mg^{2+}>Na^{+}>K^{+}$ and $HCO_3^{-}>Cl^{-}>SO_4^{2-}>NO_3^{-}$. Magnesium and sulphates charge the greatest concentration variations.

The hydrogeochemical facies of groundwater, determined using the Piper diagram [54], shows that the investigated groundwater has a homogenous distribution with bicarbonate alkaline-earth composition (Figure 4).

To assess the role of the dissolution mechanisms of carbonate compounds the relationship of HCO_3^{-} to Ca^{2+} Mg^{2+} has been verified. The observation points tend to fall above $y = x$ (dissolution of carbonates), indicating that Ca^{2+} and Mg^{2+} ions would originate from calcite and dolomite mineral dissolution in the carbonate rock areas (Figure 5).

In consideration of the geological context in which the investigated springs occur, it is to be considered that this correlation is mainly due to the dissolution of the calcium carbonate and in a minor way of the magnesium carbonate, dominant in these carbonate deposits.

The carbon dioxide of the soil reacts with water and carbonate rocks dissolving calcite and dolomite according to the following reactions:

$$\begin{aligned} CaCO_3 + 2CO_2 + 2H_2O &= 2Ca^{2+} + 4HCO_3^{-} \\ CaMg(CO_3)_2 + 2CO_2 + 2H_2O &= Ca^{2+} + Mg^{2+} + 4HCO_3^{-} \end{aligned} \quad (4)$$

In Figures 6(a) and 6(b), the saturation indices (SI) for calcite and dolomite, expressed in logarithmic form, in relation to Mg/Ca ratio are shown. Most groundwater samples are saturated or nearly saturated with respect to calcite (Figure 6(a)). On the contrary, almost all of groundwater samples are undersaturated with respect to dolomite (Figure 6(b)).

The dolomite dissolution and concurrent precipitation of calcite maintain water-mineral equilibrium (dedolomitazion) and increase Mg/Ca ratios along flow paths. The scatter plot of Na^{+} versus Cl^{-} (Figure 7) indicates that groundwater are well correlated ($r^2 = 0.75$) and show a Na/Cl ratio higher than seawater (Na/Cl = 0.86) and halite dissolution (Na/Cl = 1). The $Na^{+}/Cl^{-} > 1$ relationship may be

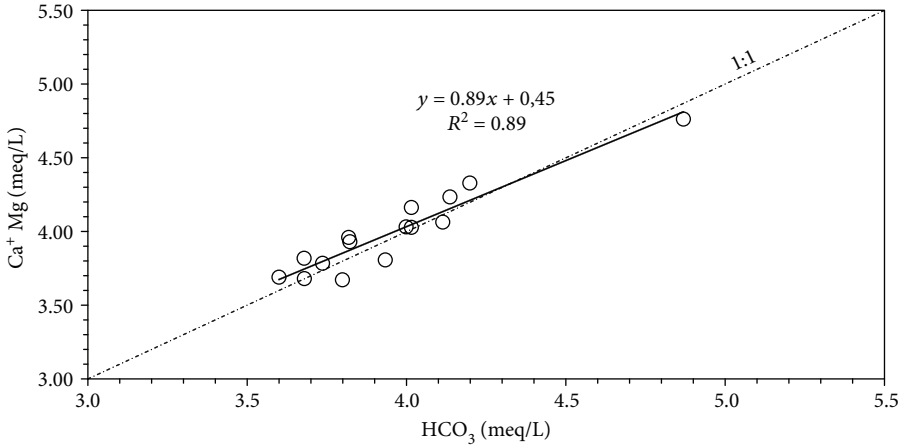

FIGURE 5: $(Ca^{2+}+Mg^{2+})$ vs. HCO_3^-. The dotted line shows the $(Ca + Mg)/HCO_3^- = 1$. The black line displays the significant correlation between selected variables.

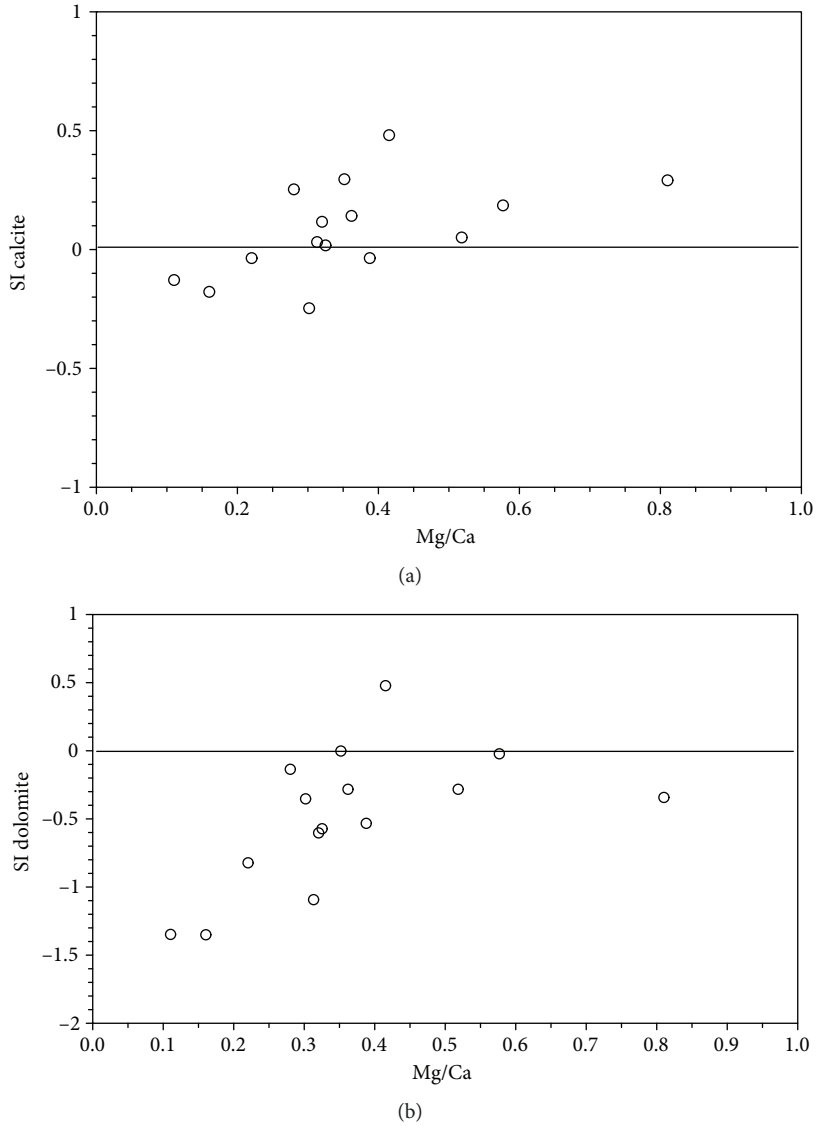

FIGURE 6: (a) Saturation index (S.I.) of calcite versus Mg/Ca ratio. (b) Saturation index (S.I.) of dolomite versus Mg/Ca ratio.

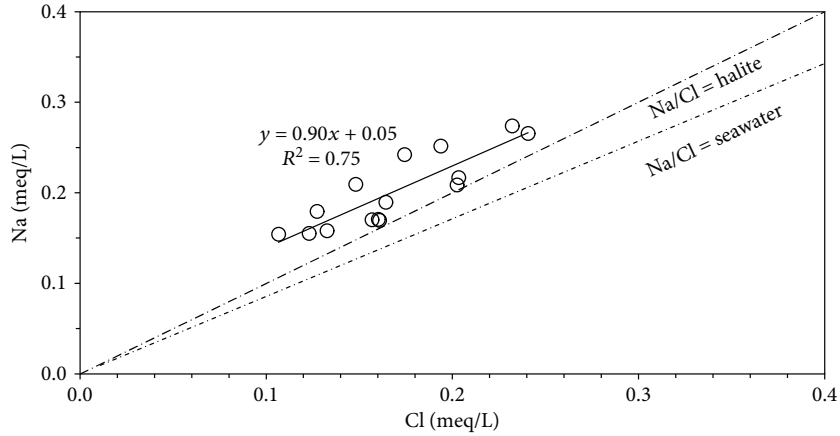

Figure 7: Na^+ vs. Cl^- in meq/L. The reference lines of the Na/Cl ratio in halite and seawater are also displayed.

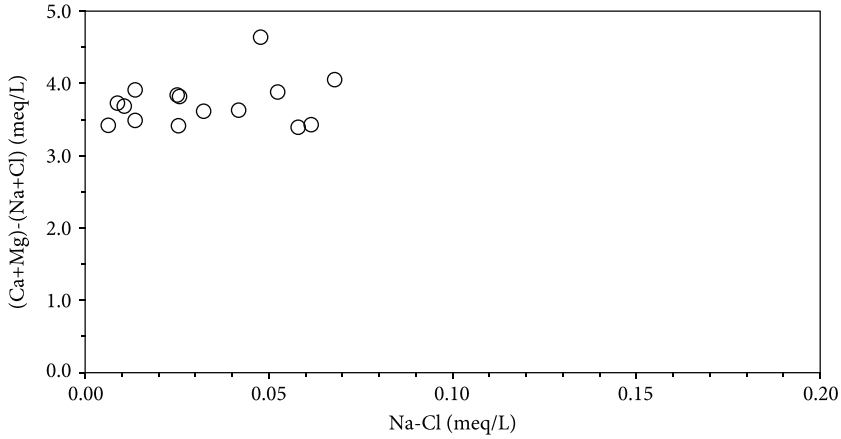

Figure 8: $[(Ca^{2+}+Mg^{2+})-(HCO_3^-+SO_4^{2-})]$ vs. (Na^+-Cl^-). The investigated water samples are not correlated highlighting that the ion exchange process does not take place.

interpreted as representative of the weathering of silicates (alkaline feldspar) or a process of ionic exchange.

In order to identify the possible process of ionic exchange, the graph of the relationship of $[(Ca^{2+}+Mg^{2+}) - (HCO_3^-+SO_4^{2-})]$ vs. (Na^+-Cl^-) has been considered (Figure 8). Ca^{2+} and Mg^{2+} concentrations are corrected by $HCO_3^-+SO_4^{2-}$, to exclude the contribution of ions from carbonates and silicates. Na^+ concentration is corrected by Cl^- to exclude Na^+ from atmospheric deposition [55].

Our data do not show a good correlation suggesting that the ionic exchange process is not possible. Therefore, the relative Na-excess is probably due to interaction of water with alkaline feldspar belonging to clastic rocks of the Frido Unit.

Factor analysis allowed verifying the important interdependences among the chemical elements. The factor component matrix (Table 4) determined by factor analysis explains the relationship between the components and the variables.

The analysis shows that component 1 is related to the sodium, sulphate, and chloride variables while electrical conductivity, calcium, potassium, and bicarbonates are linked to component 2.

The physical interpretation of the two factors is graphically evidenced in the two-component plot of Figure 9, where two main groups of variables related to physicochemical data of groundwater samples are shown and, even if they both fall within the positive value field, are anticorrelated.

In component 1, it is clear that the ions of Na^+, SO_4^{2-}, and Cl^-, even if characterized by low concentrations, have a high contribution in terms of correlation, indicating the interaction of water with silicate minerals of the arenaceous-pelitic flysch deposits. The loading of Na and Cl and their interrelation, can derive also, to a lesser extent, from the contribution of the sea spray provided by the high rainfall amounts of the study area, due to the orographic conditions and the nearness of the hydrostructure to the sea. The high permeability of the carbonate formations due to the intense fracturing state and karst processes promotes the infiltration of the precipitations into the groundwater system.

The results of component 2 indicate that the high loading factors of EC, Ca^{2+}, HCO_3^-, and K^+ can be associated with the dissolution of carbonate into the aquifer system, which increases the concentrations of these ions. Carbonate dissolution is the most important process affecting the ion concentrations of the groundwater of the samples. The loading factor of Mg^{2+} represents the processes related to the dissolution of the dolomites and dolomitic limestones.

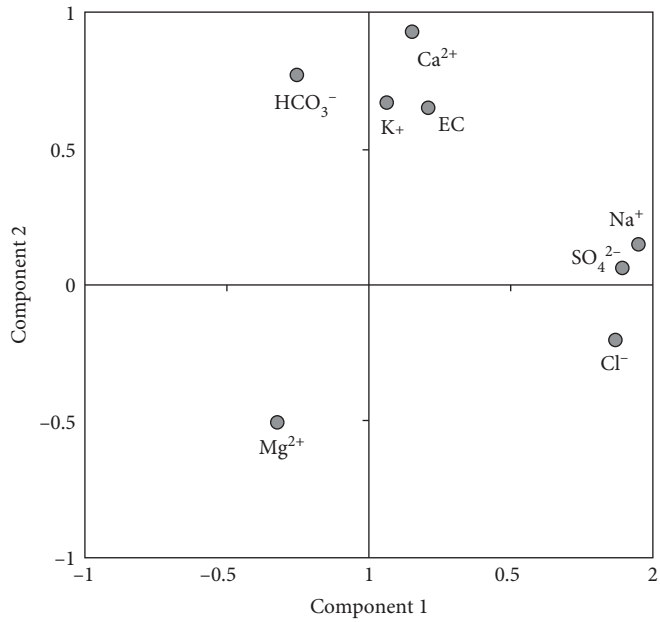

Figure 9: Factor score plot of components 1 and 2 in rotated space of the main analysed parameters.

Moreover, in the carbonate environments, in the presence of the arenaceous and marly flysch deposits, the effect of water-flysch interactions acts as the dissolution mechanisms of the silicates involving the release of detectable quantity of Ca^{2+}, HCO_3^-, Mg^{2+}, K^+, Na^+, and H_4SiO_4 [56, 57].

The factor scores of K^+ and NO_3^-, characterized by very low concentrations, do not have any discernible pattern, and the nitrate ion has no significant lithologic source; the correlation degree suggest that it may be associated mainly with zootechnical activity or surface runoff of fertilizer used for agricultural purposes.

5.2. δD and $\delta^{18}O$ Groundwater Data. Groundwater shows isotopic compositions ranging between -7.5‰ and –8.6‰ for oxygen and -42‰ and -54‰ for deuterium.

The δD and $\delta^{18}O$ relationship is plotted in Figure 10. All groundwaters plot between the Global Meteoric Water Line (GMWL) [58] and the Mediterranean Meteoric Water Line (MMWL) [59]. This indicated that groundwaters have a meteoric origin and secondary processes occurring after the precipitation (i.e., evaporation, evapotranspiration, and/or water–rock interaction) do not significantly change the isotope ratios of groundwater.

Most of the groundwater springs sampled in November 2017 show an enrichment in O and D heavier isotopes than do data measured in May 2017. The difference in $\delta^{18}O$ isotopic composition between the samplings is superior to the analytical error (0.1‰ and 1‰ for $\delta^{18}O$ and δD values, respectively). This is possible because in these springs, the contribution by seasonal rainfall is present, and this may be due to an aquifer with low water capacity and relatively short and shallow hydrogeological circuits through the sedimentary units. Only a limited number of groundwater (P10, P11, and P12 springs), sampled in November 2017, show isotopic values similar to data recorded in May 2017. These springs are not influenced by the seasonal variation of the meteoric recharge. Therefore, under these conditions we may assume that these springs drain the deep aquifers characterized by deep groundwater flow pathways, where the temporal variations of the isotopic ratios are usually within the measurement error. In addition, these groundwaters, showing mean oxygen isotope ratios between -8.4‰ and -8.6‰, are similar to the springs, located at high altitudes >900 meters above sea level (a.s.l.), and pertaining to relatively short and shallow hydrogeological circuits. This finding allows estimating that the average altitude of the recharge areas for the major springs characterized by homogenous groundwater isotopic data ranges from 900 m to 1000 m a.s.l.

6. Conclusions

This study focused on the hydrogeological setting and groundwater hydrogeochemical assessment of the carbonate hydrostructure of the Lauria Mountains northern sector (southern Apennines). The complex hydrogeological environment and the hydrodynamic characteristics of the aquifer system reflect the geostructural peculiarities of the carbonate hydrostructure. According to the stratigraphic and tectonic setting, deep groundwater flow pathways feed the major springs. The presence of these important springs plays a considerable socioeconomic role for the interest of the entire territory in terms of water availability.

Results highlight that hydrogeochemical and stable isotopic investigations are useful to defining the hydrogeological conceptual model of the aquifer system and representing the essential tool to characterize groundwater chemical assessment. Hydrogeochemical analysis elucidates that the chemical compositions of groundwater depend from the lithology and from the hydrodynamic characteristics of the systems. It suggests that carbonate dissolution is the controlling factor for groundwater chemical properties. The factor

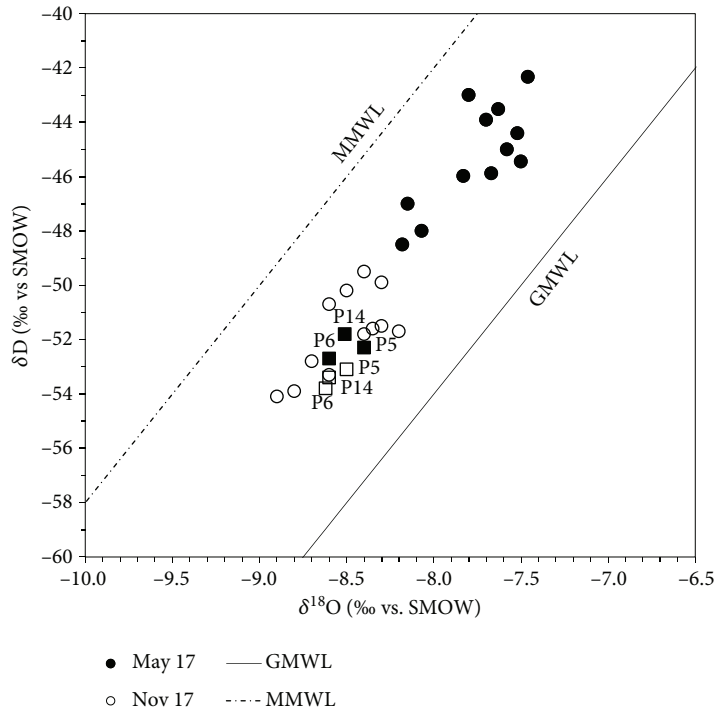

Figure 10: $\delta^{18}O$ and δD plot of local groundwater. For comparison, the global meteoric water line (GMWL) and the Mediterranean meteoric water line (MMWL) have been drawn. The filled and empty squares indicate the isotopic data of P6, P14, and P5 springs sampled in May 2017 and November 2017, respectively.

analysis has demonstrated a greater usefulness in interpreting the hydrogeochemical data relating to water–rock interaction processes with carbonate rocks and silicate minerals.

The main aim of this study was to achieve a deeper understanding of the hydrogeological system and groundwater hydrogeochemical characteristics of the carbonate hydrostructure, using a hydrogeological and hydrogeochemical integrated approach, even in hydrogeological systems with limited data availability, finalized at identifying available groundwater resources.

At present, it is possible to argue that considerable groundwater amounts can be used for supplementary and substitutive uses, or to compensate for water emergencies, through sustainable and opportune management actions and strategies.

The current changes in hydrogeology should be faced by improved focus on monitoring techniques and exploitation of information; therefore, the relevance of this carbonate hydrostructure requires further and more detailed knowledge. The findings indicate that effort should be directed, in the future, to the monitoring of the springs discharge, to the detailed isotopic study of rainfall and groundwater, for a better understanding of the preferential groundwater flow directions, of recharge time, taking into account the impact of climate change, in the perspective of protecting these resources from depletion and contamination.

Data Availability

The data used to support the findings of this study are included within the article.

Disclosure

This research was carried out in the framework of the Smart Basilicata Project, "Smart Cities and Communities and Social Innovation" (MIUR n. 84/Ric. 2012, PON 2007–2013).

Conflicts of Interest

The authors declare that there is no conflict of interest regarding the publication of this paper.

References

[1] S. Eden and R. G. Lawford, "Using science to address a growing worldwide water dilemma for the 21st century," in *Water: Science, Policy and Management. Water Resources Monograph 16*, Lawford, Ed., Publisher AGU, 2003.

[2] C. J. Vörösmarty, P. B. McIntyre, M. O. Gessner et al., "Global threats to human water security and river biodiversity," *Nature*, vol. 467, no. 7315, pp. 555–561, 2010.

[3] M. M. Mekonnen and A. Y. Hoekstra, "Four billion people facing severe water scarcity," *Science Advances*, vol. 2, no. 2, article e1500323, 2016.

[4] C. J. Vörösmarty, P. Green, J. Salisbury, and R. B. Lammers, "Global water resources: vulnerability from climate change and population growth," *Science*, vol. 289, no. 5477, pp. 284–288, 2000.

[5] T. Distefano and S. Kelly, "Are we in deep water? Water scarcity and its limits to economic growth," *Ecological Economics*, vol. 142, pp. 130–147, 2017.

[6] R. G. Taylor, B. Scanlon, P. Döll et al., "Ground water and climate change," *Nature Climate Change*, vol. 3, no. 4, pp. 322–329, 2013.

[7] European Commission, "Directive 2000/60/EC of the European Parliament and of the Council of 23 October 2000 establishing a framework for community action in the field of water policy," *Official Journal of the European Communities*, vol. 2000, 2000.

[8] European Commission, "Directive 2006/118/EC of the European Parliament and of the Council of 12 December 2006 on the protection of groundwater against pollution and deterioration," *Official Journal of the European Communities*, vol. 2006, 2006.

[9] Decreto legislativo 3 aprile 2006, *Norme in materia ambientale*, Gazzetta Ufficiale, 2006.

[10] L. W. Mays, "Groundwater resources sustainability: past, present, and future," *Water Resources Management*, vol. 27, no. 13, pp. 4409–4424, 2013.

[11] W. J. Cosgrove and D. P. Loucks, "Water management: current and future challenges and research directions," *Water Resources Research*, vol. 51, no. 6, pp. 4823–4839, 2015.

[12] I. Clark and P. Fritz, *Environmental Isotopes in Hydrology*, Lewis Publishers, New York, 1997.

[13] G. Vandenschrick, B. van Wesemael, E. Frot et al., "Using stable isotope analysis (δD–δ18O) to characterise the regional hydrology of the Sierra de Gador, south east Spain," *Journal of Hydrology*, vol. 265, no. 1-4, pp. 43–55, 2002.

[14] W. M. Edmunds, "Geochemistry's vital contribution to solving water resource problems," *Applied Geochemistry*, vol. 24, no. 6, pp. 1058–1073, 2009.

[15] I. Cartwright, T. R. Weaver, D. I. Cendón et al., "Constraining groundwater flow, residence times, inter-aquifer mixing, and aquifer properties using environmental isotopes in the southeast Murray Basin, Australia," *Applied Geochemistry*, vol. 27, no. 9, pp. 1698–1709, 2012.

[16] A. L. Herczeg, F. W. J. Leaney, M. F. Stadler, G. L. Allan, and L. K. Fifield, "Chemical and isotopic indicators of point-source recharge to a karst aquifer, South Australia," *Journal of Hydrology*, vol. 192, no. 1-4, pp. 271–299, 1997.

[17] L. Yin, G. Hou, X. Su et al., "Isotopes (δD and δ18O) in precipitation, groundwater and surface water in the Ordos Plateau, China: implications with respect to groundwater recharge and circulation," *Hydrogeology Journal*, vol. 19, no. 2, pp. 429–443, 2011.

[18] S. Prada, J. V. Cruz, and C. Figueira, "Using stable isotopes to characterize groundwater recharge sources in the volcanic island of Madeira, Portugal," *Journal of Hydrology*, vol. 536, pp. 409–425, 2016.

[19] B. D'Argenio, T. Pescatore, and P. Scandone, "Schema geologico dell'Appennino meridionale (Campania e Lucania)," in *Atti del convegno "Moderne vedute sulla geologia dell'Appennino"*, vol. 183, pp. 49–72, Quaderni Accademia Nazionale Lincei, 1973.

[20] M. Schiattarella, "Tettonica della Catena del Pollino (confine calabro-lucano)," *Memorie Società Geologica Italiana*, vol. 51, pp. 543–566, 1996.

[21] E. Perri and M. Schiattarella, "Evoluzione tettonica quaternaria del bacino di Morano Calabro (Catena del Pollino), Calabria settentrionale," *Bollettino Società Geologica Italiana*, vol. 116, pp. 3–15, 1997.

[22] M. Schiattarella, "Quaternary tectonics of the Pollino Ridge, Calabria-Lucania boundary, Southern Italy," in *Continental Transpressional and Transtensional Tectonics*, R. E. Holdsworth, R. A. Strachan, and J. F. Dewey, Eds., vol. 135, no. 1pp. 341–354, Geological Society, London, 1998.

[23] F. Russo and M. Schiattarella, "Osservazioni preliminari sull'evoluzione morfostrutturale del bacino di Castrovillari (Calabria settentrionale)," *Studi Geologici Camerti*, vol. 1992/1, pp. 271–278, 1992.

[24] E. Turco, R. Maresca, and P. Cappadona, "La tettonica pliopleistocenica del confine calabro-lucano: modello cinematico," *Memorie Società Geologica Italiana*, vol. 45, pp. 519–529, 1990.

[25] M. Schiattarella, M. M. Torrente, and F. Russo, "Analisi strutturale ed osservazioni morfostratigrafiche nel bacino del Mercure (confine calabro-lucano)," *Il Quaternario, Italian Journal of Quaternary Sciences*, vol. 7, pp. 613–626, 1994.

[26] D. Gioia and M. Schiattarella, "Caratteri morfotettonici dell'area del Valico di Prestieri e dei Monti di Lauria (Appennino Meridionale)," *Il Quaternario, Italian Journal of Quaternary Sciences*, vol. 19, no. 1, pp. 129–142, 2006.

[27] E. Patacca and P. Scandone, "Geology of the Southern Apennines," *Bollettino Società Geologica Italiana*, vol. 7, pp. 75–119, 2007.

[28] P. Scandone, "The preorogenic history of the Lagonegro basin (southern Apennines)," in *Geology of Italy*, C. Squyres, Ed., pp. 305–315, The Earth Sciences Society of the Libyan Arab Republic, 1975.

[29] P. Scandone, "Studi di geologia lucana: Carta dei terreni della serie calcareo-silico-marnosa e note illustrative," *Bollettino della Società dei Naturalisti in Napoli*, vol. 81, pp. 225–300, 1972.

[30] P. Scandone, "Studi di geologia lucana: la serie calcareo-silico-marnosa e i suoi rapporti con l'Appennino calcareo," *Bollettino Società Naturalisti in Napoli*, vol. 7766, pp. 1–175, 1967.

[31] E. Marsella, "I terreni lagonegresi tra San Fele e la Val d'Agri. Evoluzione tettonico-sedimentaria (Trias superiore-Giurassico)," in *Tesi di Dottorato in Geologia del Sedimentario*, Università di Napoli, 1988.

[32] F. Mostardini and S. Merlini, "Appennino centro meridionale. Sezioni geologiche e proposta di modello strutturale," *Memorie Società Geologica Italiana*, vol. 35, pp. 177–202, 1986.

[33] L. Ogniben, "Schema introduttivo alla geologia del confine calabro-lucano," *Memorie Società Geologica Italiana*, vol. 8, pp. 435–763, 1969.

[34] S. D. Knott, "The Liguride Complex of Southern Italy – a Cretaceous to Paleogene accretionary wedge," *Tectonophysics*, vol. 142, no. 2-4, pp. 217–226, 1987.

[35] S. D. Knott, "Structure, kinematics and metamorphism in the Liguride Complex, southern Apennines, Italy," *Journal of Structural Geology*, vol. 16, no. 8, pp. 1107–1120, 1994.

[36] S. Laurita and G. Rizzo, "Blueschist metamorphism of metabasite dykes in the serpentinites of the Frido Unit, Pollino Massif," *Rendiconti Online della Società Geologica Italiana*, vol. 45, pp. 129–135, 2018.

[37] G. Rizzo, M. T. C. Sansone, F. Perri, and S. Laurita, "Mineralogy and petrology of the metasedimentary rocks from the Frido Unit (southern Apennines, Italy)," *Periodico di Mineralogia*, vol. 85, pp. 153–168, 2016.

[38] G. Papani, M. T. De Nardo, G. Bettelli, D. Rio, C. Tellini, and L. Vernia, *Note Illustrative della Carta Geologica d'Italia alla*

scala 1:50.000 e Foglio 521 LAURIA, ISPRA, Servizio Geologico d'Italia, 2016.

[39] G. Bonardi, F. O. Amore, G. Ciampo, P. De Capoa, P. Miconnet, and V. Perrone, "Il Complesso Liguride Auct.: stato delle conoscenze e problemi aperti sulla sua evoluzione pre-appenninica ed i suoi rapporti con l'Arco Calabro," *Memorie Società Geologica Italiana*, vol. 4, pp. 17–35, 1988.

[40] F. Canora, M. A. Musto, and F. Sdao, "Groundwater recharge assessment in the carbonate aquifer system of the Lauria Mounts (southern Italy) by GIS-based distributed hydrogeological balance method," in *Computational Science and Its Applications–ICCSA 2018, Lecture Notes in Computer Science*, O. Gervasi, Ed., Springer, 2018.

[41] M. Civita, "Proposte operative per la legenda delle carte idrogeologiche," *Bollettino Società Naturalisti in Napoli*, vol. 82, pp. 1–12, 1973.

[42] F. Sdao and G. D'Ecclesiis, "Idrogeologia dei Monti di Lauria (Basilicata)," in *Atti del 3° Convegno Nazionale Protezione e Gestione Acque Sotterranee per il III Millennio*, P. Bologna, Ed., vol. 2, pp. 175–183, Quaderni di Geologia Applicata, Parma, 1999.

[43] M. C. Dichicco, A. De Bonis, G. Mongelli, G. Rizzo, and R. Sinisi, "μ-Raman spectroscopy and X-ray diffraction of asbestos' minerals for geo-environmental monitoring: the case of the southern Apennines natural sources," *Applied Clay Science*, vol. 141, pp. 292–299, 2017.

[44] M. Dichicco, S. Laurita, R. Sinisi, R. Battiloro, and G. Rizzo, "Environmental and health: the importance of Tremolite Occurence in the Pollino Geopark (Southern Italy)," *Geosciences*, vol. 8, no. 3, p. 98, 2018.

[45] G. Rizzo, S. Laurita, and U. Altenberger, "The Timpa delle Murge ophiolitic gabbros, southern Apennines: insights from petrology and geochemistry and consequences to the geodynamic setting," *Periodico di Mineralogia*, vol. 87, pp. 5–20, 2018.

[46] Landsystem, *Piano di Risanamento delle Acque della Regione Basilicata: Censimento dei corpi idrici*, Regione Basilicata, 1990.

[47] L. Ferranti, J. S. Oldow, and M. Sacchi, "Pre-Quaternary orogen-parallel extension in the Southern Apennine belt, Italy," *Tectonophysics*, vol. 260, no. 4, pp. 325–347, 1996.

[48] A. Ietto and B. D'Argenio, "Some accounts on thrust and subsequent extensional tectonics in the Pollino Mountains. Southern Apennines," *Rendiconti Online Società Geologica Italiana*, vol. 13, pp. 121–124, 1990.

[49] D. L. Parkhurst and C. A. J. Appello, "User's guide to PHREEQC (version 2)—a computer program for speciation, batch-reaction, one-dimensional transport, and inverse geochemical calculations," *US Geological Survey Water-Resources Investigations*, pp. 99–4259, 1999, Report.

[50] D. L. Parkhurst and C. A. J. Appello, "Description of input and examples for PHREEQC version 3: a computer program for speciation, batch-reaction, one-dimensional transport, and inverse geochemical calculations," in *Techniques and Methods, Book 6, chapter A43*, p. 497, U.S. Geological Survey, 2013.

[51] A. Shrivastava and V. B. Gupta, "Methods for the determination of limit of detection and limit of quantitation of the analytical methods," *Chronicles of Young Scientists*, vol. 2, no. 1, pp. 21–25, 2011.

[52] Statgraphics® Centurion XVI User Manual, *StatPoint Technologies, Inc*, 2009.

[53] Decreto legislativo 2 febbraio 2001, *Attuazione della direttiva 98/83/CE relativa alla qualità delle acque destinate al consumo umano*, Gazzetta Ufficiale, 2001.

[54] A. M. Piper, "A graphic procedure in the geochemical interpretation of water-analyses," *Transactions of the American Geophysical Union*, vol. 25, no. 6, pp. 914–923, 1944.

[55] A. Biswas, B. Nath, P. Bhattacharya et al., "Hydrogeochemical contrast between brown and grey sand aquifers in shallow depth of Bengal Basin: consequences for sustainable drinking water supply," *Science of The Total Environment*, vol. 431, pp. 402–412, 2012.

[56] E. Merlak, *Solubilità della silice nell'interazione acqua-flysch del carso Triestino*, vol. 44, Atti e Memorie della Commissione Grotte E. Boegan, 2014.

[57] M. Amanti, M. Buchetti, D. Centioli et al., "Hydrogeochemical features of spring waters in the Sheet N. 348 "Antrodoco" area," *Periodico di Mineralogia*, vol. 81, no. 3, pp. 269–299, 2012.

[58] H. Craig, "Isotopic variations in meteoric waters," *Science*, vol. 133, no. 3465, pp. 1702-1703, 1961.

[59] J. R. Gat and I. Carmi, "Evolution of the isotopic composition of atmospheric waters in the Mediterranean Sea area," *Journal of Geophysical Research*, vol. 75, no. 15, pp. 3039–3048, 1970.